ELECTRON COOLING EXPERIMENTS AT S-LSR

T. Shirai#, S. Fujimoto, M. Ikegami, H. Tongu, M. Tanabe, H. Souda, A. Noda
ICR, Kyoto-U, Uji, Kyoto, Japan,
K. Noda, NIRS, Anagawa, Inage, Chiba, Japan,
T. Fujimoto, S. Iwata, S. Shibuya, AEC, Anagawa, Inage, Chiba, Japan,
E. Syresin, A. Smirnov, I. Meshkov, JINR, Dubna, Moscow Region, Russia
H. Fadil, M. Grieser, MPI Kernphysik, Saupfercheckweg, Heidelberg, Germany

Abstract

The electron cooler for S-LSR was designed to maximize the cooling length in the limited drift space of the ring. The effective cooling length is 0.44 m, while the total length of the cooler is 1.63 m. The one-dimensional ordering of protons is one of the subjects of S-LSR. Abrupt jumps in the momentum spread and the Schottky noise power have been observed for protons at a particle number of around 2000. The beam temperature was 0.17 meV and 1 meV in the longitudinal and transverse directions at the transition, respectively. The normalized transition temperature of protons is close to those of heavy ions at ESR. The lowest momentum spread below the transition was 1.4×10^{-6}, which corresponded to the longitudinal beam temperature of 26 μeV (0.3 K). It is close to the longitudinal electron temperature.

INTRODUCTION

S-LSR is a compact ion storage/cooler ring at Kyoto University to study physics of cooled ion beams and applications of beam cooling. S-LSR has an electron beam cooler and a laser cooling system. The laser cooling system has been developed for the study of the crystalline beam [1] and the laser cooling experiments have been carried out since 2007 [2].

The commissioning of the electron cooling was started from October 2005. The 7 MeV proton beam from the linac was used and the first cooling was observed on October 31. The proton and electron beam current were 50 μA and 60 mA, respectively. The initial momentum spread of 4×10^{-3} was reduced to 2×10^{-4} after the cooling. The initial beam size of 26 mm was reduced to 1.2 mm.

In 2006 and 2007, the following experiments have been carried out using the electron cooling:

- Development of the induction accelerator sweep cooling for the hot ion beam with large momentum spread [3].
- Short pulse generation using the electron cooling and the RF phase rotation [4].
- Study of the coherent instability of the electron cooled proton beam with high intensity and the damping by the feedback system [5].
- One-dimensional ordering experiments of electron cooled protons [6, 7].

In this paper, the electron cooler at S-LSR is introduced at first. Figure 1 shows the cross-sectional view of the electron cooler and table 1 shows the main parameters of S-LSR and the electron cooler. Then, the results of the one-dimensional ordering of protons are mainly reported.

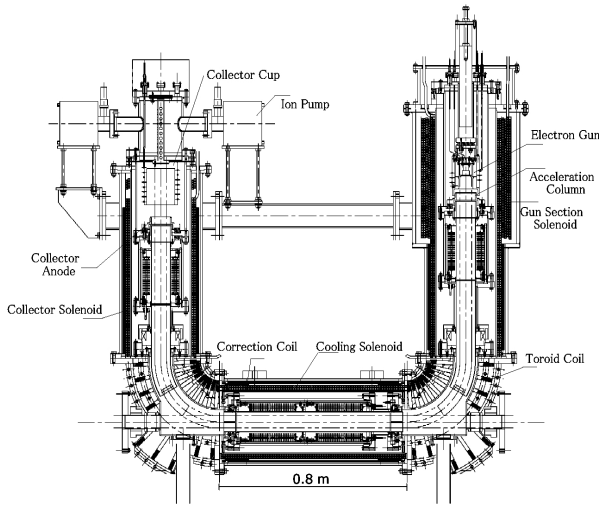

Figure 1: Cross-sectional view of the electron cooler at S-LSR.

Table 1: Main parameters of S-LSR and the electron cooler.

Ring	
Circumference	22.557 m
Length of Drift Space	1.86 m
Number of Periods	6
Average Vacuum Pressure	1×10^{-8} Pa
Electron Cooler	
Maximum Electron Energy	5 keV
Electron Beam Current	25 mA - 300 mA
Beam Diameter	50 mm
Solenoid Field in the central	500 Gauss
Expansion Factor	3
Cooler Solenoid Length	800 mm
Effective Cooling Length	440 mm

#shirai@kyticr.kuicr.kyoto-u.ac.jp

ELECTRON COOLER

The design issues of the electron cooler at S-LSR were a high cooling force and a compactness in order to install the short drift space (1.86 m). The following design methods and devices were adopted:

- Precise three-dimensional magnetic field simulation of the whole system of the cooler using TOSCA [8].
- High perveance electron gun. The typical perveance is 2.3 μP [8].
- Small toroid radius (0.25 m) and the elliptical vacuum chamber in the central solenoid for the compactness of the toroid section.
- Six vertical correction coils in the central solenoid in order to extend the effective cooling length.
- Electrostatic deflectors in the toroid coils in order to compensate the drift motion of the electron beam [9].

Using the vertical correction coils, the effective length of the cooling section becomes 440 mm, while the lengths of the cooler solenoid and the overall electron cooler are 0.80 m and 1.63 m, respectively. The electrostatic deflectors reduce a secondary electron loss. Figure 2 shows the electron loss rate and the maximum cooling force with various deflector voltages in the toroid. The cooling force was measured by the induction accelerator. When the deflector voltage was changed, the dipole magnetic field in the toroid was also changed to keep the electron orbit constant. When the voltage was 1.25 kV, there was no dipole magnetic field for the compensation. The loss rate is reduced with the deflectors, while the cooling force is almost constant. It shows that the electron temperature gets no effect from the electrostatic potential. The small change of the cooling force was induced by the vertical closed orbit distortion due to the dipole magnetic field in the toroid.

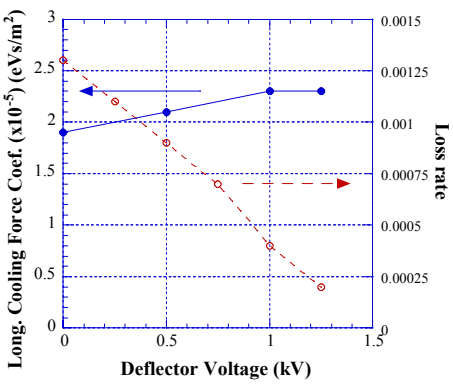

Figure 2: Longitudinal cooling force coefficient in the linear region and the electron loss rate with various deflector voltages with the electron current of 107mA.

The systematic cooling force measurements have been carried out to evaluate the cooler. The ion is 7 MeV proton and the induction accelerator is used. Figure 3(a) shows the cooling force at the electron current of 25, 50 and 100 mA. The cooling forces have maximum values at the relative velocity of around 4000 m/sec. It shows that the electron temperature is almost constant between 25 mA and 100 mA. Figure 3(b) shows the electron current dependence of the maximum longitudinal cooling force. The cooling force is proportional to the electron current.

Figure 4 shows the comparison between the measured longitudinal cooling force and the cooling force model at the electron current of 100 mA. The electron temperature is assumed to be 40 μeV in the models. The measured one is different by a factor of 10 from the magnetized and non-magnetized cooling models. It is about two times smaller than the Parkhomchuk's formula [10].

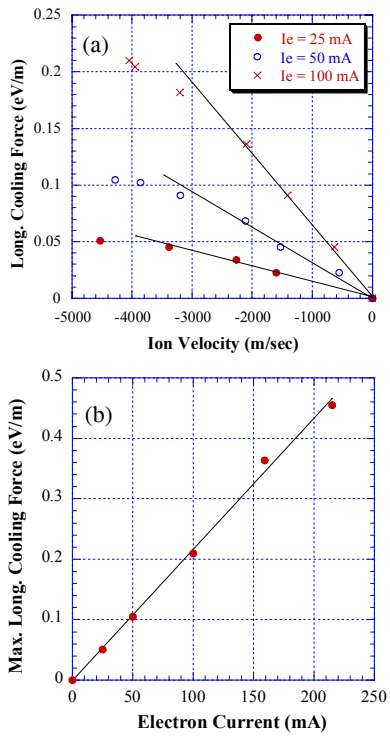

Figure 3 (a): Longitudinal cooling force with the electron current of 25, 50 and 100 mA (2.2, 4.4 and 8.8x10^6 e$^-$/cm^3) as a function of the relative ion velocity. (b): Electron current dependence of the maximum longitudinal cooling force.

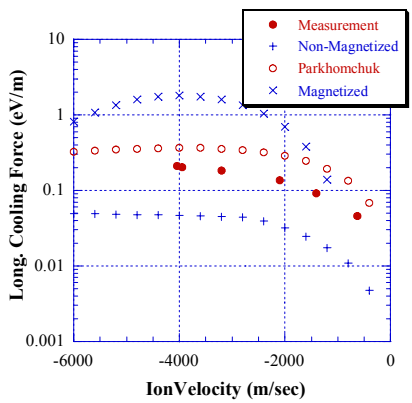

Figure 4: Comparison between the measured longitudinal cooling force and the cooling force models, such as non-magnetized, Parkhomchuk and magnetized cooling model. The electron current is 100 mA (8.8x10^6 e$^-$/cm^3).

ONE-DIMENSIONAL ORDERING FOR PROTONS

The ion ordering by the electron cooling was reported at NAP-M [11] and the abrupt jump of the momentum spread was found at ESR for highly charged heavy ions [12]. The similar jump of the momentum spread was also confirmed at CRYRING for other heavy ions [13]. However, the jump of the momentum spread has not been found for protons. The parameters of the one-dimensional ordering experiments for protons at S-LSR are shown in Table 2.

Table 2: Parameters of the one-dimensional ordering experiments for protons.

Beam	Proton, 7 MeV
Revolution frequency	1.61 MHz
Lifetime with cooling	1.7 x 10^4 sec
Ring	
Betatron tune	(1.645, 1.206)
Max. β-function	(3.9 m, 3.2 m)
Max. dispersion	1.8 m
Electron Cooler	
Energy	3.8 keV
Beam Current	25, 50, 100 mA
Expansion Factor	3

Experimental Setup

In the one-dimensional ordering experiment, a momentum spread and an emittance of the cooled beam were measured as a function of a particle number. Since the typical particle number at the ordering transition was expected to be some thousands, special beam diagnostics were necessary for such very low intensity, especially for singly charged protons.

The particle number was measured by the two independent methods. One is an ionization residual gas monitor and the other is a bunch signal monitor. The results of the two methods agree within 10 % from 10^8 to 500 protons. The momentum spread was measured from the frequency spread of the Schottky noise spectrum. A helical pickup was used for the measurement, which had been developed for the storage ring, TARN at INS, Tokyo University [14]. Figure 5 shows the schematic view of the electrode. It is a travelling-wave type electrode and the phase velocity of the electric signal coincides with the ion velocity (7 MeV proton).

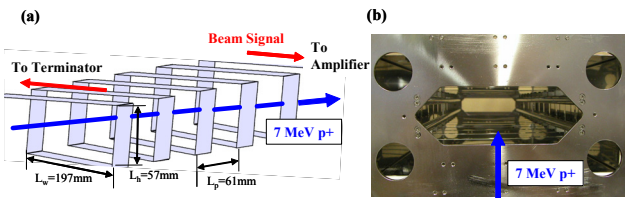

Figure 5 (a): Schematic view of the helical electrode. (b): Photo of the helical pickup.

The beam radius was measured by a beam scraper. At first, the protons of 10^8 was injected and cooled. The typical beam diameter was around 1 mm. The scraper was moved into the circulating beam and stopped at a certain position for 0.1 second, and then removed back away. It killed a part of the beam and reduced the particle number. The rms beam radius σ was determined from the distance L between the scraper position and the beam centre. The ratio between L and σ was calculated by the beam simulation using BETACOOL code [15] and it was found to be 3.5.

Momentum Spread Measurement

Figure 6(a) shows momentum spreads of the protons as a function of the particle numbers in the ring. The electron current was 25 mA, 50 mA and 100 mA. The momentum spread is defined as 1σ of the fitted Gaussian function to the momentum distribution. The momentum spread is proportional to $N^{0.29}$ above a particle number of 4000. At the particle number of around 2000, the momentum spread drops abruptly. The transition momentum spread at the electron current of 25 mA is 3.5×10^{-6}, which corresponds to the ion temperature of 0.17 meV. It is considered that this abrupt drop is evidence of ordering of the protons. The lowest momentum spread below the transition is 1.4×10^{-6}, which corresponds to the longitudinal ion temperature of 26 μeV (0.3 K). It is close to the longitudinal electron temperature.

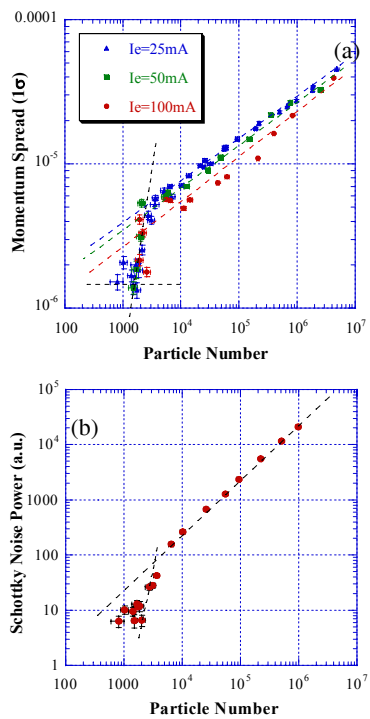

Figure 6(a): Momentum spread as a function of the particle numbers with three different electron currents, 25 mA, 50 mA and 100 mA. (b): Schottky noise power as a function of a particle numbers with electron current of 25 mA. The Schottky noise power is defined as the integrated area of the spectrum [6].

Figure 6(b) shows the Schottky noise power as a function of the particle number with an electron current of 25 mA. It is proportional to $N^{0.99}$ above a particle number of 6000. At the transition point, it drops by one order of magnitude. Similar phenomena have been observed for highly charged heavy ions at CRYRING [13].

Transverse Beam Size Measurement

The transverse beam temperature can be estimated from the beam size measurements. Figure 7 shows the measured horizontal beam size as a function of the particle numbers. The beam size was measured by the ionization residual gas monitor and the beam scraper. The electron current of the cooler was 25 mA. The beam radius is proportional to $N^{0.28}$, and monotonically decreased. The beam radius is 17 μm at a particle number of 4000, which is the transition point of the momentum spread. It is impossible to determine whether there is an abrupt jump of the beam size, because of the insufficient resolution of the scraper. The corresponding horizontal emittance is $1.7\text{x}10^{-4}$ π.mm.mrad with the β-function of 1.7 m at the scraper. If it is assumed that the horizontal and vertical emittances were equal, the transverse temperature is 1 meV. On the other hand, the transverse electron temperature is 34 meV with the expansion factor of 3. The transverse proton temperature of 1 meV is much smaller than that of the electron. It is the result of the magnetized cooling [16] and the key for the ordering of the proton beam.

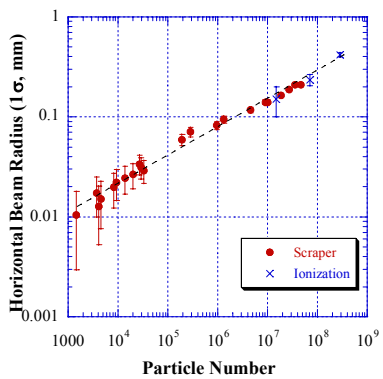

Figure 7: Horizontal beam radius as a function of the particle numbers with electron current of 25 mA. They were measured by the scraper and the ionization residual gas monitor [6].

Heavy ions and Proton

The conditions of the one-dimensional ordering for heavy ions are explained by the reflection probability between two particles [17]. The momentum spread of the heavy ions has a transition at the reflection probability between 60 % and 80 % [18]. In order to compare the heavy ions and proton, the normalized temperature was introduced as the following definition [18],

$$\widehat{T}_{//,\perp} = \frac{2}{m_i c^2}\left(2r_i \beta\gamma \frac{\nu}{R}\right)^{-2/3} k_B T_{//,\perp}, \qquad (1)$$

where m_i is the mass of the ion, r_i is the classical ion radius, βγ is the relativistic factor, ν is the betatron tune and R is the average radius of the ring. Table 3 shows the transition temperatures and normalized ones for the proton at S-LSR [6] and for the heavy ions at ESR [19]. Although the transition temperatures are different by a factor of 1000 between U^{92+} and p^+, the normalized transition temperatures are very close and both have the similar reflection probabilities [6]. It suggests that the transition of the momentum spread occurs by the same mechanism from highly charged heavy ions to proton. It is a general phenomenon for the ion beam. The low transverse ion temperature by the magnetized cooling is the essential condition of the ordering for the light ions, because the transverse transition temperature is usually lower than the transverse electron temperature.

Table 3: Transition temperatures and the normalized temperatures for heavy ions and proton.

Ions	$T_{//}$	$T_{\perp}$	$\widehat{T}_{//}$	$\widehat{T}_{\perp}$
p^+ [6]	0.17 meV	1 meV	1.2	6.5
C^{6+} [19]	4.0 meV	11 meV	0.62	1.6
Zn^{30+}[19]	78 meV	0.64 eV	0.78	7.6
U^{92+} [19]	470 meV	3.4 eV	0.70	5.1

Beam Simulation

The molecular dynamics simulations were carried out for the proton ordering to analyze more precisely. The program code was BETACOOL [15] and the electron cooling was treated as the constant cooling rate, which was calculated from the cooling force measurements. Figure 8(a) shows the trajectories in the cooling process on the phase space of the horizontal emittance and the momentum spread. The particle numbers are 2000 and 6000, respectively. In both cases, the beams are cooled down along the similar trajectories but the beam at the particle number of 6000 stops at the point with the momentum spread of $6\text{x}10^{-6}$. It reaches the equilibrium state, where the electron cooling rate and the IBS heating rate are equal. On the other hand, the momentum spread at the particle number of 2000 decreases monotonically and there is no limit of the lowest momentum spread. The reduction rate of the momentum spread is almost the same as the input cooling rate.

Figure 8(b) shows the final momentum spread obtained by the molecular dynamic simulation with various particle numbers. The measured momentum spread is also shown in the same figure. The momentum spread drops at the particle number of 4000 in the simulation, while it drops between the particle number of 4000 and 2000 in the measurement. The simulation is globally consistent with the measurement.

These simulations suggest that the cooling rate is close to the maximum IBS heating rate with the particle number of 4000. At the particle number of 2000, the cooling rate

exceeds the maximum heating rate. Concerning the transition, the mechanism in the one-dimensional ordering is similar to that of the crystalline beam. This result also explains why the one-dimensional ordering occurs at the very small particle number. Because of the small cooling rate of the electron cooling, it can exceed the IBS heating rate only with the very small particle number. It is different from the crystalline beam simulation by laser cooling. The laser cooling has a high cooling rate and can overcome the intrabeam scattering even with the large particle number.

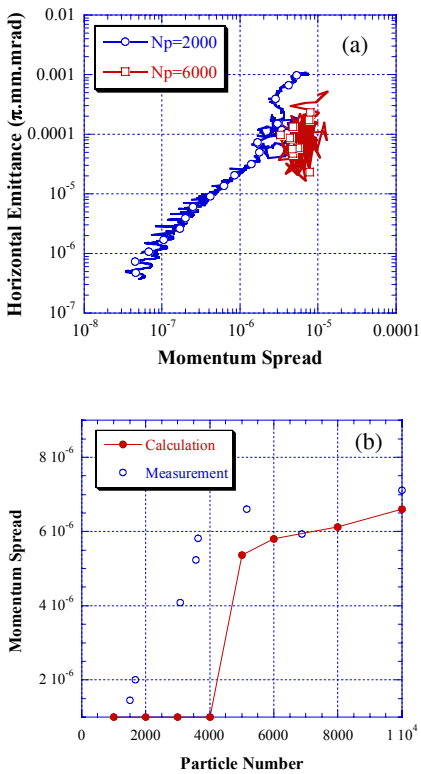

Figure 8(a): Beam trajectories in the cooling process on the phase space of the horizontal emittance and the momentum spread. The particle number is 2000 and 6000. (b): Final momentum spread obtained by the molecular dynamic simulation with various particle numbers. The measured momentum spread is also shown in the figure.

ACKNOWLEDGEMENTS

This work was supported by the Advanced Compact Accelerator Development project by MEXT of the Japanese Government and 21st Century COE at Kyoto University - Diversity and Universality in Physics.

REFERENCES

[1] J. P. Schiffer and P. Kienle, "Could there be an ordered Condensed State in Beams of Fully Stripped Heavy Ions", Zeitschrift for Physik A, **321** (1985) p.181.

[2] A. Noda et al., "Present Status and Recent Activity on Laser Cooling at S-LSR", in Proceedings of this workshop.

[3] H. Fadil et al., "Electron Beam Cooling Experiments at S-LSR", HIMAC Report-111 (2006).

[4] T. Fujimoto et al., "Fast extraction of the short bunched proton beam for investigation of free radicals behaviour", to be submitted to Jpn. J. Appl. Phys.

[5] S. Fujimoto et al., "Feedback Damping of a Coherent Instability at Small-Laser Equipped Storage Ring, S-LSR", Jpn. J. Appl. Phys., **45** (2006) p.1307.

[6] T. Shirai et al., "One dimensional beam ordering of protons in a storage ring", Phys. Rev. Lett., **98** (2007) 204801.

[7] A. Smirnov et al., "Necessary Condition for Beam Ordering", in Proceedings of this workshop.

[8] H. Fadil et al., "Design of a compact electron cooler for the S-LSR", Nucl. Instrum. Methods Phys. Res. Sect. A, **532** (2004) p.446.

[9] V. V. Parkhomchuk, "Development of a New Generation of Coolers with a Hollow Electron Beam and Electrostatic Bending", Proc. of COOL05, Galena (2005) p.249.

[10] V. V. Parkhomchuk, "New insights in the theory of electron cooling", Nucl. Instrum. Methods Phys. Res. Sect. A, **441** (2000) p.9.

[11] V. V. Parkhomchuk, "Physics of Fast Electron Cooling", Proc. of ECOOL84, Karlsruhe (1984) p.71.

[12] M. Steck et al., "Anomalous Temperature Reduction of Electron-Cooled Heavy Ion Beams in the Storage Ring ESR", Phys. Rev. Lett., **77** (1996) p.3803.

[13] H. Danared et al., "Model and Observations of Schottky-Noise Suppression in a Cold Heavy-Ion Beam", Phys. Rev. Lett., **88** (2002) 174801.

[14] H. Yonehara et al., "Equipments For Momentum Cooling at TARN", INS Report No. INS-NUMA-49, (1983).

[15] I. Meshkov et al., "Physics guide of BETACOOL code Version 1.1", BNL Note C-A/AP/262 (2006).

[16] Ya. S. Derbenev and A. N. Skrinsky, "The Physics of Electron Cooling", Physics Reviews (Soviet Scientific Reviews), **3** (1981) p.165.

[17] R. W. Hasse, "Theoretical Verification of Coulomb Order of Ions in a Storage Ring", Phys. Rev. Lett., **83** (1999) p.3430.

[18] H. Okamoto et al., "One-dimensional Ordering of Ultra-Low-Density Ion Beams in a Storage Ring", Phys. Rev. E, **69** (2004) 066504.

[19] M. Steck et al., "Electron cooling experiments at the ESR", Nucl. Instrum. Methods Phys. Res. Sect. A, **532** (2004) p.357.